

Organogels

Boron Effect on Sugar-Based Organogelators

Andreas D. Ludwig, [a] Arnaud Saint-Jalmes, [b] Cristelle Mériadec, [b] Franck Artzner, [b] Olivier Tasseau, [a] Fabienne Berrée, *[a] and Loïc Lemiègre*[a]

Abstract: The reaction of several alkylglucosides with phenyl boronic acid permitted easy access to a series of alkylglucoside phenyl boronate derivatives. This type of compound has structures similar to those of known benzylidene glucoside organogelators except for the presence of a boronate function in place of the acetal one. Low to very low concentrations of these amphiphilic molecules produced gelation of several organic solvents. The rheological properties of the corresponding soft materials characterized them as elastic solids. They were further characterized by SEM to obtain

more information on their morphologies and by SAXS to determine the type of self-assembly involved within the gels. The sensitivity of the boronate function towards hydrolysis was also investigated. We demonstrated that a small amount of water (5% v/v) was sufficient to disrupt the organogels leading to the original alkylglucoside and phenyl boronic acid; an important difference with the stable benzylidene-based organogelators. Such water-sensitive boronated organogelators could be suitable substances for the preparation of smart soft material for topical drug delivery.

Introduction

The preparation of gels with low-molecular-weight gelators is possible thanks to weak intermolecular interactions such as van der Waals interactions, π - π interactions, hydrogen bonding or electrostatic interactions.^[1] The corresponding self-assembly turns aqueous or organic solutions into hydrogels or organogels, respectively. This important area of research provides soft materials that find various types of application in oil remediation,^[2] nanotube formation,^[3] drug delivery^[4] or sensitive materials. [5] Typical gelators are based on sugars, lipids, peptides and aromatics, which usually provide the required weak interactions. Sugar-based structures are often suitable for the preparation of hydrogels if the hydrophilicity of the carbohydrate is well balanced with hydrophobic tails. [6] Usually access to sugar-based organogelators requires further functionalization of the sugar moiety with the introduction of aromatic rings, acyl or alkyl chains, most of the time by creation of C-O linkages.^[7] However, sugars in general, and glucoside derivatives in particular, are known to react selectively with boronic acids leading to corresponding boronic esters. [8] Several strategies have been developed for the detection of sugars or for the formation of molecular self-assembly, thanks to this easy and efficient reaction. [8a,9] In regard to the specific case of glucoside derivatives, the boronic acid promotes the esterification of the hydroxy functions available on the 4- and 6-positions of the glucoside.^[10] Boronic esters have already been involved in organogelator structures,[11] but only few examples have taken advantage of this function for the preparation of sugar-based organogelators.^[12] One important illustration related to our research work was described by Shimizu et al.[12b-d] who designed a luminescent organogelator based on a glycolipid naphthyl boronic ester. We described herein a series of alkylglucoside phenylboronic esters 1 (Figure 1) easily prepared in a single chemical step. Their chemical structures are similar to known benzylidene type organogelators 2 that already demonstrated their ability as good organogelators with typical minimum gelation concentration between 2 to $10 \ \text{mg} \ \text{mL}^{-1}.^{[7e,j,13]}$ The replacement of the acetal function by a boronic ester group induces two main differences; 1) the tetrahedral carbon is replaced by a planar boron atom and 2) the presence of a vacant orbital on the boron atom. As a consequence, the geometry of the molecule, and therefore its selfassembling properties, are supposed to dramatically change. Furthermore, the easier hydrolysis of the boronate function compared with the acetal one might conduce to water-sensitive self-assembly. However, one could imagine that this slight

[b] Dr. A. Saint-Jalmes, C. Mériadec, Dr. F. Artzner CNRS, IPR (Institut de Physique de Rennes)—UMR 6251 Université de Rennes, 35000 Rennes (France)

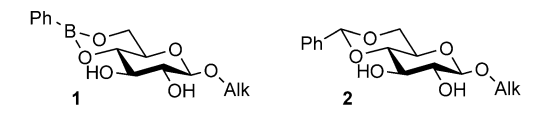


Figure 1. Alkylglucoside phenyl boronic esters 1 and known benzylidene glucoside organogelators 2.

[[]a] A. D. Ludwig, O. Tasseau, Dr. F. Berrée, Dr. L. Lemiègre Ecole Nationale Supérieure de Chimie de Rennes, CNRS, ISCR—UMR6226 Université de Rennes, 35000 Rennes (France) E-mail: fabienne.berree@univ-rennes1.fr loic.lemiegre@ensc-rennes.fr

Supporting information and the ORCID identification number(s) for the author(s) of this article can be found under: https://doi.org/10.1002/chem.202001970.



difference would prevent these less-stable boronate derivatives from providing gelation of organic solvents. Within this new family of organogelators, we investigated the impact of the alkyl chain length on the gelation of various solvents. The organogels were characterized at a macroscopic scale by rheology (mechanical properties, stability), at a microscopic scale by scanning electron microscopy (SEM) and molecular level was achieved by small angle X-ray scattering (SAXS) analysis. In addition, their sensitivity against water was confirmed.

Results and Discussion

The synthesis of boronic esters 1 was simply achieved by mixing equimolar amounts of alkylglucosides 4 and phenylboronic acid 3 without solvent. Elimination of water by heating under high vacuum displaced the equilibrium towards the formation of the final product (Scheme 1). Complete reactions were observed for alkylglucosides 4a-h within 15 minutes at 90 °C whatever the alkyl tail equipping the glucoside (methyl, n-butyl, n-hexyl, n-heptyl, n-octyl, n-nonyl, n-decyl and n-dodecyl chains). All boronic esters 1a-h were isolated without purification or after simple washing with diisopropyl ether in excellent yields (84-99%) and purities. This series of boronic esters with a broad range of hydrophilic/lipophilic balance, was further engaged in gelation assays with various solvents. The α -butyl derivative α -1 **b** was also prepared in the same manner (not shown) in order to investigate the stereochemical impact of the nature of the glycosidic bond (α or β).

To evaluate the potential of this series of new molecules as organogelators, we first selected several solvents covering different solvation behaviors. Toluene represents an example of aromatic solvent, cyclohexane is a typical cycloalkane, ethyl myristate and isopropyl palmitate are interesting bio-based solvents used in cosmetic applications and topical drug delivery. [4a] Table 1 gathers the results for each molecule/solvent combination. For each case, we determined if the molecule was insoluble even after heating (I), soluble after heating (S), behave as an opaque gel (G^O), as a transparent gel (G^T) or as a precipitate upon cooling (P; photos of representative gels are available in the Supporting Information). The first member of the series (methyl, 1 a) was not soluble whatever the solvent used (Table 1, entry 1). This shortest chain length did not provide a sufficient hydrophilic/lipophilic balance to permit the gelation of the solvents considered here. Concerning the stereochemistry of the glycosidic bond, if the α isomer α -1 **b** (entry 2) did not provide organogel either in toluene or in cyclohexane, conversely, the β isomer β -1 **b** (entry 3) was able to

Scheme 1. Synthesis of alkylglucoside boronic esters 1 a-h.

myristate palmitate 1 β-p-methyl 1a I I I I I 2 α -p-n-butyl α -1b P I n.d. (b) n.d. (b) 3 β -p-n-butyl β -1b G^T 11 G^T 3 G^T 10 G^T 11 4 β -p-n-hexyl 1c G^0 10 I G^0 10 G^0 10 5 β -p-n-heptyl 1d G^T 9 P G^T 9 G^0 9 6 β -p-n-octyl 1e G^0 12 I G^0 8 G^0 12 7 β -p-n-nonyl 1f G^0 12 G^0 4 G^0 12 G^0 11	Table 1. Gelation assays. ^[a]								
$ \begin{array}{cccccccccccccccccccccccccccccccccccc$		Compound	Toluene	СуН	,	Isopropyl palmitate			
8 β-D- <i>n-</i> αecyl i g 3 G 10 G 10	3 4 5 6	α -D- n -butyl α -1 b β -D- n -butyl β -1 b β -D- n -hexyl 1 c β -D- n -heptyl 1 d β -D- n -octyl 1 e	G ^T 11 G ^O 10 G ^T 9 G ^O 12	I P I	G ^T 10 G ^O 10 G ^T 9 G ^O 8	G ^T 11 G ^O 10 G ^O 9 G ^O 12			

[a] I: Insoluble; S: Soluble; P: Precipitate; G^P : Partial gel; G^T : Translucent gel; G^O : Opaque gel. Values indicate minimum gelation concentrations (MGC) in mg mL $^{-1}$. [b] Not determined.

gel the four solvents giving translucent organogels with toluene, cyclohexane and fatty esters. Indeed, stereochemistry is an important feature that dramatically changes the geometry of molecules and therefore their ability to self-assemble. [14] For the rest of the study, we only considered β isomers and evaluated the impact of the length of the alkyl chain on the gelation properties (entries 3-9). Indeed, the length of the alkyl chain had a remarkable influence on the gelation properties. n-Butyl derivative β -1 b led to organogels with the all four solvents at low to very low concentrations (3 to 11 mg mL⁻¹; entry 3). The addition of two carbon atoms (n-hexyl 1c, entry 4) provided very similar minimum gelation concentrations (MGC) for the four solvents. Middle chain length (nheptyl, **1 d** and *n*-octyl, **1 e**; entries 5–6) led to organogels in all solvents except cyclohexane for which precipitation or insolubility were obtained. The *n*-nonyl derivative **1 f** did not lead to a full gelation except for ethyl myristate (entry 7). Increasing even more the chain length reduced the solubility in cyclohexane, increased the solubility in toluene but provided transparent organogels in fatty ester solvents at low concentrations (10 mg mL $^{-1}$; n-decyl **1 g**, entry 8). Surprisingly, the n-dodecyl counterpart 1 h (entry 9) had a different behavior in cyclohexane providing an organogel at a very low concentration (2 mg mL⁻¹) and in only one of the two fatty esters (isopropyl palmitate).

Mechanical properties were investigated by rheological amplitude-sweep. Graphs of G' and G'' against strain percentage are shown in Figure 2 (data shown for β -n-butyl derivative, graphs of other organogels are available in the Supporting Information). Experiments were performed with a frequency of 1 Hz at the MGC described in Table 1.

Under such conditions, at low strains, all organogels exhibited storage moduli greater than loss moduli (Table 2). It demonstrates that the gels can be considered as elastic solids, but rather soft ones. Indeed, their elastic moduli reach only values from hundreds to a few thousands of Pa, and they remain only a few times larger than the viscous moduli. Interestingly the β -n-butyl derivative β -1b provided the largest G' and G'/G'' values after gelation of toluene (Table 2, entry 1). The n-dodecyl derivative 1h induced the formation of stiffer gels in cyclo-

Chem. Eur. J. **2020**, *26*, 13927 – 13934 **www.chemeurj.org** 13928 © 2020 Wiley-VCH GmbH

1g (n-Dec), 1h (n-Dodec)

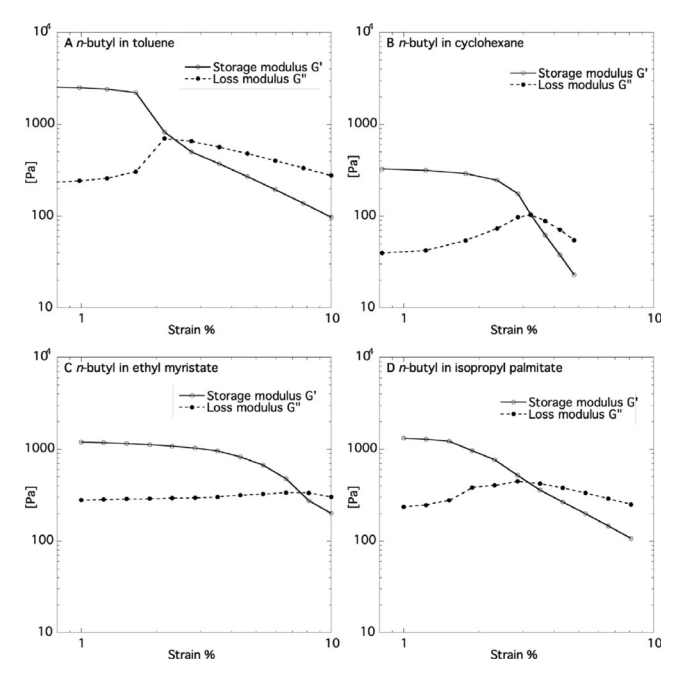


Figure 2. Storage modulus (G', full line) and loss modulus (G'', dashed line) against strain % of organogels obtained with β -n-butyl β -1 **b** in A) toluene, B) cyclohexane, C) ethyl myristate and D) isopropyl palmitate.

Table 2. Storage and loss modulus at low strain of organogels.							
	Compound	Solvent	Storage modulus [Pa] ^[a]	Loss modulus [Pa] ^[a]	<i>G'/G''</i> ^[a]		
1	β- D - <i>n</i> -butyl β- 1 b	Tol	2724	213	12.8		
2	β- D - <i>n</i> -butyl β- 1 b	CyH	326	40	8.1		
3	β- D - <i>n</i> -butyl β- 1 b	EM	1196	279	4.3		
4 β-p-n-butyl β- 1b IP 1322 234 5.6							
5 β-p-n-hexyl 1 c Tol 706 111 6.4							
6	·						
7	β-D- <i>n</i> -hexyl 1 c	IP	449	140	3.2		
8	β- D - <i>n</i> -heptyl 1 d	Tol	1181	98	12.1		
9	β-ɒ- <i>n</i> -heptyl 1 d	EM	3023	199	15.2		
10	β- D - <i>n</i> -heptyl 1 d	IP	837	103	8.1		
11	β-D- <i>n</i> -octyl 1 e	Tol	753	341	2.2		
12	β-D- <i>n</i> -octyl 1 e	EM	1075	287	3.7		
13	β-D- <i>n</i> -octyl 1 e	IP	540	104	5.2		
14	β-ם- <i>n</i> -nonyl 1 f	EM	126	45	2.8		
15	β-D- <i>n</i> -decyl 1 g	EM	2762	346	8.0		
16	β-D- <i>n</i> -decyl 1 g	IP	1487	126	11.8		
17	β-D- <i>n</i> -dodecyl 1 h	СуН	429	35	12.3		
18	β-D- n -dodecyl 1 h	IP	722	154	4.7		
[a] A	[a] At strain < 1%, 1 Hz frequency.						

hexane (Table 2, entry 17) and *n*-heptyl **1d** and *n*-decyl **1g** counterparts afforded stiffer gels (larger elastic moduli) in fatty ester solvents (Table 2, entries 9, 15, 16). These observations might result from different tightness of packing of organogelator fibers within the solvent. Then interaction of the fibers with the solvent molecules would vary for each organogelator/solvent couple. Indeed, long-chain fatty ester solvents are reasonably more compatible with long-chain organogels whereas short-chain organogelators would express a more aromatic behavior, more compatible with toluene for instance.

At high amplitudes of deformation, a same qualitative behavior is found for all the organogels: above a deformation threshold (typically ranging from 1 to 10%), the samples provide a viscous response to the mechanical solicitation, eventually dominating the elastic one (G'' > G'). In the case of β -nbutyl derivative β -1 b, above amplitudes of around 2%, some first plastic rearrangements are induced inside the organogels, decreasing the elastic modulus G'. At amplitudes above 2.5 to 8%, the elasticity of the organogel vanished, with G' collapsing down to G". Under such amplitudes, the organogel structure could not effectively sustain the deformation and the sample started to irreversibly flow. Similar conclusions raised from the analysis of the other organogels (see the Supporting Information). An experiment at 2% amplitude and 1 Hz frequency showed constant moduli over a period of 2 h (Figure 3 A). Thus, the constant rheological properties obtained under such conditions demonstrated the stability of the organogels over time. In addition, consecutive amplitude-sweep experiments on a same gel also showed that the low strain regime was independent of the number of measurements, but that the deformation threshold (where G' becomes smaller than G'') was dramatically modified after the first run (runs from the black line to red lines, Figure 3B) and then continuously by the repetition of tests (from red lines to blue and then green lines, Figure 3 B). This implies that the first self-assembled structures obtained through the gelation process were irreversibly modified each time that they were deformed over their deformation threshold (Figure 3B and the Supporting Information). Reorganization of the fiber network might occur during the deformation of the organogels.

Toluene and cyclohexane-based organogels were freezedried and the corresponding xerogels were analyzed by scanning electron microscopy (SEM; Figure 4). The morphology of xerogels originated from toluene revealed characteristic networks of fibers entangled one to another in the case of *n*-butyl, *n*-hexyl and *n*-octyl derivatives (Figures 4A, B, D, E). However, dense structures corresponding to a bundle of fibers were observed in the case of *n*-heptyl counterpart (Figure 4C). This exception would find its origin in the odd number of carbon atoms within the alkyl chain compared to the even

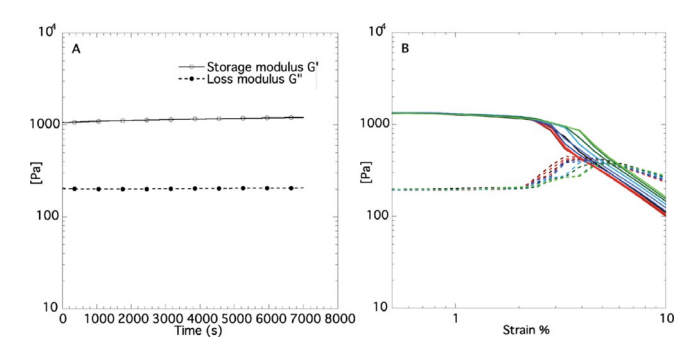


Figure 3. A) Storage modulus (G', full line) and loss modulus (G'', dashed line) against time (frequency = 1 Hz and amplitude = 2%). B) Ten successive amplitude-sweep experiments (first experiment in black, then red, blue, and green lines). Storage modulus (G', full line) and loss modulus (G'', dashed line) for the gel of β-n-butyl β-1 b in isopropyl palmitate (IP).



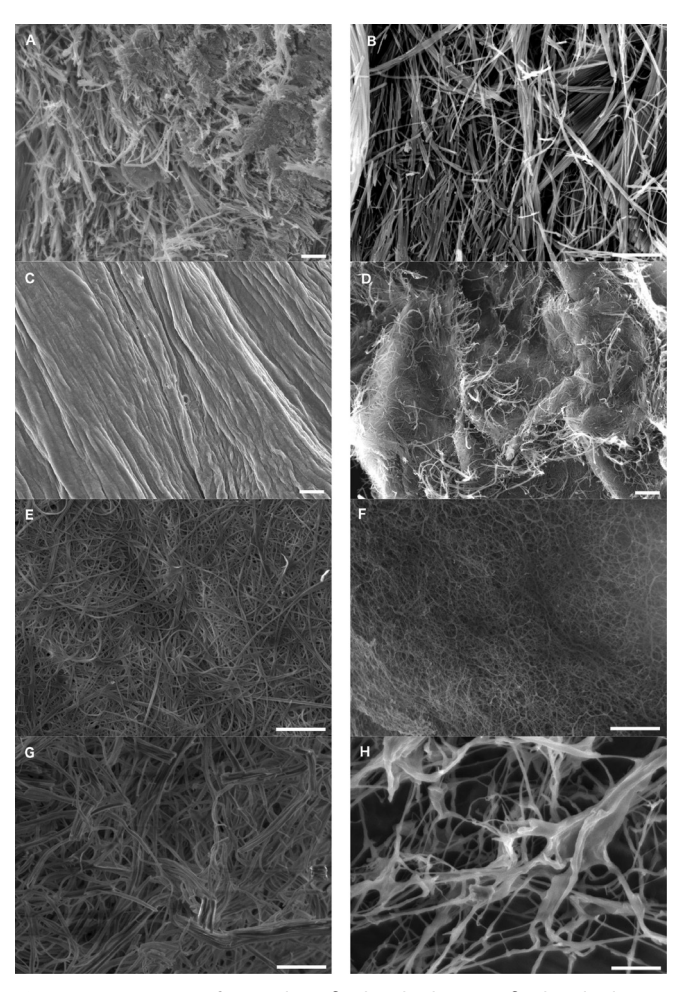


Figure 4. SEM images of xerogels. A) β-n-butyl/toluene, B) β-n-hexyl/toluene, C) β-n-heptyl/toluene, D) β-n-octyl/toluene, E) β-n-octyl/toluene, F) β-n-butyl/cyclohexane, G) β-n-nonyl/cyclohexane, H) β-n-dodecyl/cyclohexane). Scale bar: 10 μ m.

number of carbon atoms for the other organogelators. The SEM images of xerogels obtained from cyclohexane (Figure 4F–H) also revealed fibrillar networks for *n*-butyl (Figure 4F) and *n*-nonyl (Figure 4G) derivatives whereas *n*-dodecyl derivative led to a network involving large clusters of fibers (Figure 4H).

The fibrillar networks observed by SEM originate from the self-assembly of the organogelators within the solvent. To better understand the type of self-assembly involved during gelation, we embarked on a small angle X-ray scattering (SAXS) study of some members of the series. Measurements were successfully achieved for organogels obtained in toluene with β -D-octyl **1e** (Figure 5) and β -D-hexyl **1c** (Supporting Information). Figure 5 compares SAXS profiles of the organogel at 20 mg mL⁻¹ of **1e** in toluene (blue) and the corresponding xerogel (red). Both organogel and xerogel have the same scattering profiles. Indexations revealed the existence of a hexagonal phase exhibiting a 3D crystal packing (Table 3). This hexagonal phase was assigned without any ambiguity and consequently, tracing q_{hkl} in a hexagonal lattice, where h, k, and lrefer to Miller indices, gave access to repeating parameters of a = 26.8 Å and c = 5.47 Å.

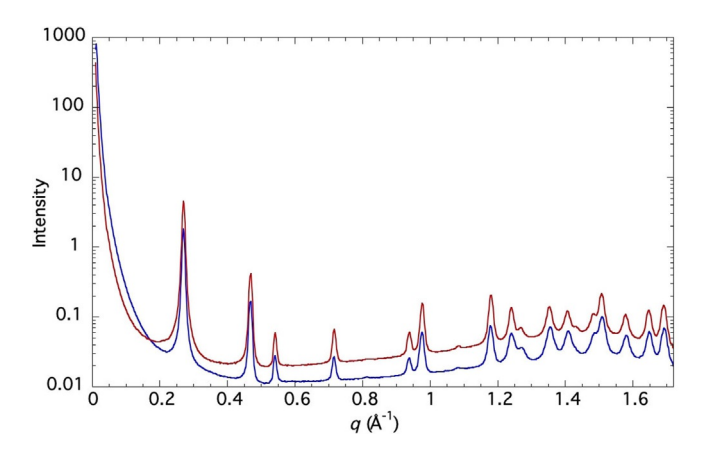


Figure 5. SAXS profiles of organogel in toluene (blue) and xerogel obtained with β -n-octyl **1e** (red).

			ndexations of 26.8 Å, $c = 5.47$		nal phase
(h, k, l)	q _{calc} [Å ⁻¹]	$q_{ m obs}$ [Å $^{-1}$]	(h, k, l)	<i>q</i> _{calc} [Å ⁻¹]	q _{obs} [Å ⁻¹]
(1, 0, 0) (1, 1, 0) (2, 0, 0) (2, 1, 0) (2, 2, 0) (3, 1, 0) (3, 2, 0) (4, 1, 0)	0.2710 0.4693 0.5419 0.7169 0.9387 0.9770 1.1811 1.2417	0.2709 0.4696 0.5424 0.7172 0.9397 0.9774 1.1811 1.2415	(2, 0, 1) (5, 0, 0) (3, 3, 0) (2, 2, 1) (5, 1, 0) (4, 0, 1) (4, 3, 0)	1.2705 1.3548 1.4080 1.4837 1.5087 1.5796 1.6482	1.2709 1.3544 1.4075 1.4830 1.5085 1.5801 1.6482

The unit cell volume is 3390 ų and molecular weight of 1e is 378 g mol $^{-1}$. With a density of 1.11, the number of molecules per unit cell is 6. The molecules may be localized on any position of the hexagonal lattice. It is simpler to imagine three sets of dimers centered on the C_2 axes (Figure 6A, B). This dimer must exhibit smaller areas at both ends to fit in the center of the hexagonal phase and a larger area at its center to accommodate the space available (Figure 6B). This type of organization can be compared to self-assemblies involved in cylindrical micelles. [15]

This in mind, a compatible dimer structure involves: 1) disorganized alkyl chains at both ends which fit into the center of the hexagonal phase and 2) interdigitated aromatic rings at the center of the dimer. Several types of packing can be envisaged based on the interaction between aromatic rings: face to face or edge to face including T-shaped geometry or herringbone packing. The later fits the best with the repeating parameter c (5.47 Å; Figure 6 C). Indeed, edge-to-face stacking (Tshaped geometry) would have led to a wrong orientation of the two members of the dimer and face-to-face stacking would have required a larger repeating parameter (= 7 Å). It is also noteworthy that the herringbone packing was previously observed within the crystal packing of a similar boronate derivative (methyl-2-deoxy- α -D-glucopyranoside 4,6-phenylboronate). [16] Thus, Figure 6C (extended chains are shown for clarity) represents the possible structure of the dimer, its vertical pack-

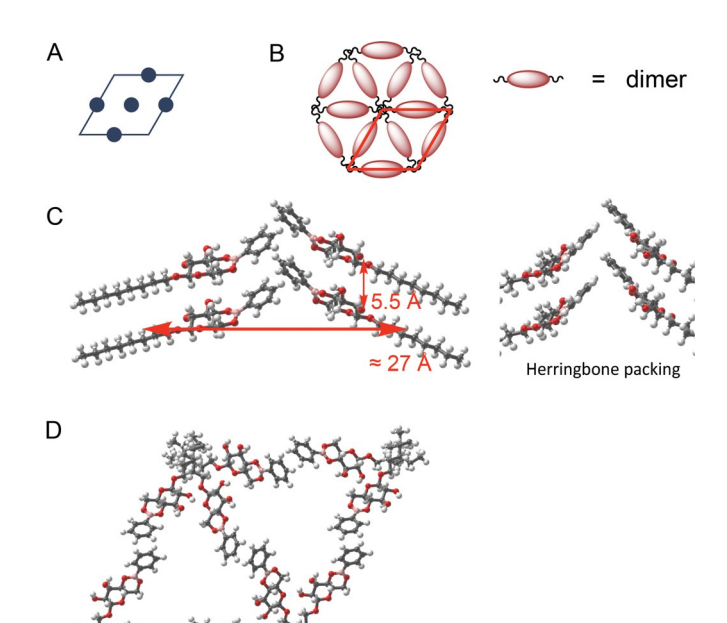


Figure 6. Representation of the hexagonal packing characterized by SAXS for 1 e. A) distribution of five dimers (6 molecules) within the unit cell; B) self-assembly of dimers within the hexagonal phase and global shape of the dimer; C) self-assembly of four molecules and herringbone packing; D) self-assembly of ten molecules within the unit cell.

ing and interdigitation of aromatic rings in respect of parameter c (5.47 Å). Figure 6D represents the possible packing of three dimers within the hexagonal phase, the alkyl chain being disorganized in the center of each hexagon in respect of parameters a (26.8 Å). A very similar self-assembly was characterized for the organogel obtained with β -D-hexyl $1\,\mathrm{c}$. However, the scattering profile exhibited a liquid crystal state instead of the 3D crystal packing. This hexagonal phase was also assigned without any ambiguity (see the Supporting Information). A comparable parameter (a=28.7 Å) found its origin from a similar packing model (Figure 6D), the less crystallinity of the liquid crystal state would explain the slight difference between the parameters a of $1\,\mathrm{e}$ and $1\,\mathrm{c}$ in favor of $1\,\mathrm{c}$.

The sp² hybridization of a boron atom of a boronate function induces a planar geometry, whereas the sp³ hybridization of the carbon atom of an acetal function confers a tetrahedral geometry. It triggers a dramatic difference between the two organogelators 1 and 2 (Figure 7). Indeed, the particular geometry of the boronate function offers a different orientation of the aromatic ring in regard to the sugar moiety. Therefore, this orientation impacts the global shape of the molecule and is then responsible for the type of packing observed here and characterized by SAXS.

As mentioned in the introduction, boronate functions are usually sensitive to aqueous media whereas benzylidene functions are stable in the presence of water, at least at neutral pH. Thus, we evaluated the behavior of the organogels obtained with the n-butyl derivative $1\,b$ selected as an example of the series. The organogels in toluene, ethyl myristate and isopropyl palmitate were exposed to water $(5\% \ v/v)$ at room tempera-

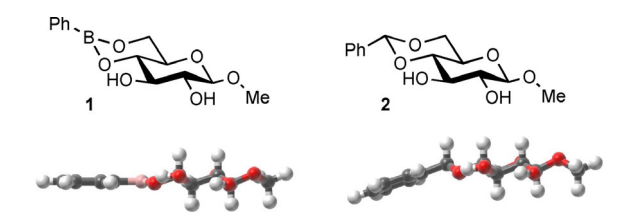


Figure 7. Representation of the impact of boronate and acetal geometries on the orientation of the aromatic rings. (Minimization obtained at an AM1 level.)

ture during the time of the experiment. Until 1 h, the gels were partially disrupted with most of the material being in a gel state, between 1 h and 3 h, the gels loosed their structures towards a fluid state with some pieces of gel still present and after 3 h, the gel state of all samples totally disappeared leading to biphasic or monophasic solutions depending on the solvent used for the formation of the gels (Figure 8). We also repeated the same experiments (gel from β -butyl β -1 b in toluene) except that we replaced fresh distilled water by acetate buffer (pH 4.8) or carbonate buffer (pH 9.8). Very similar results were obtained after addition of 5% v/v of these two buffer solution.

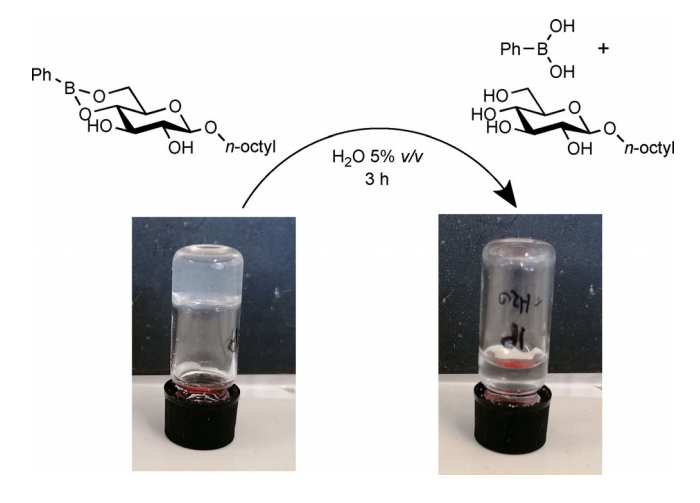


Figure 8. Water sensitivity of organogels: disruption of a gel by adding water (5 % v/v) by hydrolysis of the boronate function. (Images shown for isopropyl palmitate case.)

The 1 H NMR analysis of the water phase confirmed the hydrolysis of the organogelator into its two original components; phenylboronic acid and n-butyl- β -D-glucoside (Figure 9). It confirmed the water sensitivity of the boronate function which is then responsible for the disruption of the organogel.

Conclusions

A series of glycolipid phenylboronic esters was easily prepared in one step from alkylglucosides and phenylboronic acid. These new amphiphilic structures revealed good gelation abilities for the four typical organic solvents evaluated in this study (toluene, cyclohexane, fatty esters). The rheological properties

Chem. Eur. J. **2020**, *26*, 13927 – 13934 **www.chemeurj.org** 13931 © 2020 Wiley-VCH GmbH

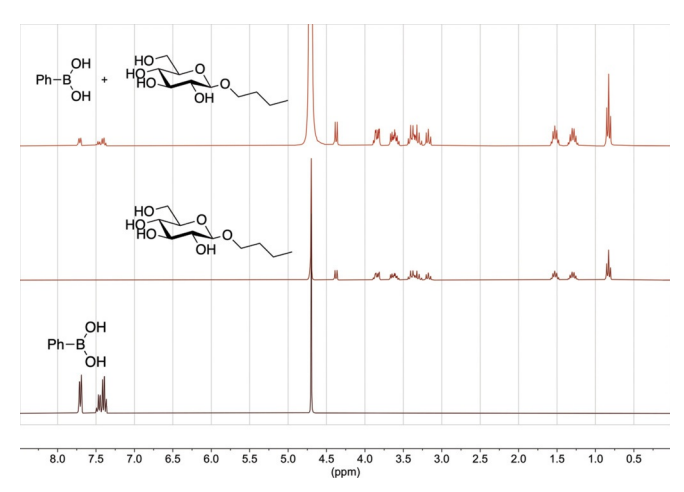


Figure 9. ¹H NMR spectra in D_2O of phenylboronic acid (bottom), *n*-butyl-β-p-glucoside (middle) and water phase after disruption of the organogel (β-1 **b** in toluene) with 5 % v/v of water (top).

and morphologies of the organogels were determined for each gel obtained with all possible solvent/organogelator combinations. It showed that the alkyl chain length on the glucoside played an important role on the gelation ability of the different solvents. The organogelators self-assembled within the solvent to form fibers observed by SEM. These fibers were the result of the packing of organogelators in a hexagonal lattice where they behave as dimers. In addition to the preparation and characterization of these organogels, we demonstrated that the addition of a small amount of water (5% v/v) was enough to disrupt the organogels in few hours (less than 3 h). The mechanism of disruption is clearly related to the hydrolysis of the boronate function. Therefore, the introduction of a boron atom within the structure of these organogelators deeply impacts and enriches the properties of the so formed organogels. For instance, these soft materials represent useful systems for topical drug delivery with controlled release upon contact with aqueous media. Such applications and tuning of the water sensitivity are now under investigation in our laboratories.

Experimental Section

General information

¹H NMR spectra (300 MHz, 400 MHz), ¹³C NMR (75 MHz, 101 MHz) and ¹¹B (96 MHz) were recorded on Bruker AC 300 and AC 400 spectrometers. Chemical shifts are given in ppm and coupling constants J in Hz. Multiplicities are presented as follows: s=singlet, d=doublet, t=triplet, q=quartet, quint=quintuplet, hex=hexuplet, m=multiplet, br=broad. The carbon bearing the boron atom was not observed due to the quadrupolar relaxation mechanism of ¹¹B nucleus. High-resolution mass spectra (HRMS) were recorded, either on a Bruker MaXis 4G, an Agilent 6510, or a Thermo Fisher Q-Exactive spectrometer (Centre Régional de Mesures Physiques de l'Ouest, Rennes) using positive ion Electron-Spray ionization techniques. Melting points were measured on a melting point apparatus Stuart SMP10 and are uncorrected. Specific rotation [deg cm³ q⁻¹] was measured on a PerkinElmer-341 polarimeter.

General procedure for the synthesis of boronic esters 1

In a 25 mL round bottom flask, alkylglucoside (0.3 mmol) and phenylboronic acid (37 mg, 0.3 mmol) were added. The mixture was then stirred in a kugelrohr distillation apparatus at 90 °C; under 0.1 mm Hg for 15 min to give the product pure enough to make gels. Compounds were washed by diisopropyl ether when necessary.

Methyl-β-p-glucopyranoside 4,6-phenylboronate $1 a.^{(17)}$ 143 mg (99%); white solid; m.p. = 188–190 °C. [α]_D = -21 (C 0.2, CH₂Cl₂).
¹H NMR (300 MHz, CDCl₃): δ = 7.81 (d, J = 7.2 Hz, 2 H), 7.46 (t, J = 7.4 Hz, 1 H), 7.36 (t, J = 7.4 Hz, 2 H), 4.38 (d, J = 7.7 Hz, 1 H, H₁), 4.32 (dd, J = 10.4, 5.4 Hz, 1 H, H₆), 4.01 (t, J = 10.3 Hz, 1 H, H₆), 3.85–3.70 (m, 2 H, H₃ H₄), 3.60 (s, 3 H), 3.58–3.49 (m, 2 H, H₂ H₅), 2.80 (d, J = 1.8 Hz, 1 H, OH), 2.55 ppm (d, J = 2.3 Hz, 1 H, OH). ¹³C NMR (75 MHz, CDCl₃): δ = 134.3, 131.4, 127.8, 104.4 (C₁), 75.1 (C₄), 74.7 (C₂), 74.3 (C₃), 68.7 (C₅), 64.2 (C₆), 57.7 ppm (OCH₃). The carbon α to the boron was not observed. ¹¹B NMR (96 MHz, CDCl₃): δ = 28.7 ppm. HRMS (ESI⁺) [M+Na]⁺ calculated for C₁₃H₁₇O₆¹¹BNa 303.10159, found 303.1011.

Butyl-β-D-glucopyranoside 4,6-phenylboronate β-1 **b**: 134 mg (98%); white solid; m.p.=153-155 °C; [α]_D=-87 (C 1, CH₂Cl₂). ¹H NMR (300 MHz, CDCl₃): δ =7.80 (d, J=7.1 Hz, 2H), 7.44 (t, J=7.4 Hz, 1 H), 7.35 (t, J=7.5 Hz, 2 H), 4.43 (d, J=7.7 Hz, 1 H, H₁), 4.30 (dd, J=10.4, 5.4 Hz, 1 H, H₆), 4.00 (t, J=10.4 Hz, 1 H, H₆), 3.92 (dt, J=9.5, 6.8 Hz, 1 H, OCH₂), 3.83-3.70 (m, 2 H, H₃ H₄), 3.63-3.50 (m, 3 H, OCH₂ H₅ H₂), 2.95 (s, 1 H, OH), 2.67 (d, J=2.4 Hz, 1 H, OH), 1.63 (quint, J=6.8 Hz, 2 H), 1.41 (hex, J=7.3 Hz, 2 H), 0.94 ppm (t, J=7.3 Hz, 3 H). ¹³C NMR (75 MHz, CDCl₃): δ =134.1, 131.2, 127.6, 103.2 (C₁), 74.9 (C₃), 74.5 (C₄), 74.1 (C₂), 70.3 (OCH₂), 68.6 (C₅), 64.1 (C₆), 31.6, 19.1, 13.8 ppm. The carbon α to the boron was not observed. ¹¹B NMR (96 MHz, CDCl₃): δ =26.8 ppm. HRMS (ESI⁺) [M+Na]⁺ calculated for C₁₆H₂₃O₆ ¹¹BNa 345.1485, found 345.1481.

Butyl-α-p-glucopyranoside 4,6-phenylboronate α-1 b: 115 mg (84%); white solid; m.p. = 100–102 °C. [α]_D = +95 (C 1, CH₂Cl₂). ¹H NMR (400 MHz, CDCl₃): δ = 7.81 (d, J = 7.1 Hz, 2 H), 7.45 (t, J = 7.3 Hz, 1 H), 7.34 (t, J = 7.4 Hz, 2 H), 4.91 (d, J = 3.9 Hz, 1 H, H₁), 4.22 (dd, J = 9.2, 4.2 Hz, 1 H, H₆), 3.94 (t, J = 10.4 Hz, 1 H, H₆), 3.90–3.85 (m, 2 H, H₅ H₃), 3.79–3.69 (m, 2 H, OCH₂ H₄), 3.66 (dd, J = 9.4, 3.9 Hz, 1 H, H₂), 3.50 (dt, J = 9.8, 6.5 Hz, 1 H, OCH₂), 1.61 (quint, J = 6.9 Hz, 2 H), 1.43–1.34 (m, 2 H), 0.93 ppm (t, J = 7.4 Hz, 3 H). ¹³C NMR (101 MHz, CDCl₃): δ = 134.3, 131.3, 127.7, 98.9 (C₁), 75.0 (C₄), 73.6 (C₃), 72.7 (C₂), 68.7 (OCH₂), 64.7 (C₅), 64.5 (C₆), 31.6, 19.5, 13.9 ppm. The carbon α to the boron was not observed. ¹¹B NMR (96 MHz, CDCl₃): δ = 27.2 ppm. HRMS (ESI⁺) [M+Na]⁺ calculated for C₁₆H₂₃O₆¹¹B Na 345.14854, found 345.1480.

Hexyl-β-D-glucopyranoside 4,6-phenylboronate 1 c: 103 mg (98%); white solid; m.p.=173–175 °C. [α]_D=-40 (C 1, CH₂Cl₂). ¹H NMR (300 MHz, CDCl₃): δ =7.81 (dd, J=7.1, 1.3 Hz, 2H), 7.45 (tt, J=7.3, 1.4 Hz, 1H), 7.36 (t, J=7.3 Hz 2H), 4.44 (d, J=7.7 Hz, 1H, H₁), 4.30 (dd, J=10.4, 5.4 Hz, 1H, H₆), 3.85–3.73 (m, 2H, H₃ H₄), 3.61–3.50 (m, 3H, OCH₂ H₂ H₅), 2.85 (d, J=1.9 Hz, 1H, OH), 2.56 (d, J=2.4 Hz, 1H, OH), 1.64 (quint, J=7.5 Hz, 2H), 1.41–1.27 (m, 6H), 0.90 ppm (t, J=6.8 Hz, 3H). ¹³C NMR (75 MHz, CDCl₃): δ =134.3, 131.3, 127.8, 103.4 (C1), 75.1 (C2), 74.7 (C4), 74.3 (C3), 70.8 (OCH2), 68.7 (C5), 64.2 (C6), 31.7, 29.7, 25.7, 22.7, 14.2 ppm. The carbon α to the boron was not observed. ¹¹B NMR (96 MHz, CDCl₃): δ =27.7 ppm. HRMS (ESI⁺) [M+Na]⁺ calculated for C₁₈H₂₇O₆¹¹BNa 373.1798, found 373.1796.

Heptyl-β-p-glucopyranoside 4,6-phenylboronate 1d: 103 mg (99%); white solid; m.p. = 164–166 °C. [α]_D = -54 (C 1, CH₂Cl₂). ¹H NMR (300 MHz, CDCl₃): δ = 7.84 (d, J = 6.5 Hz, 2 H), 7.46 (t, J = 7.4 Hz, 1 H), 7.37 (t, J = 7.2 Hz, 2 H), 4.45 (d, J = 7.7 Hz, 1 H, H₁), 4.31 (dd, J = 10.4,



5.3 Hz, 1 H, H₆), 4.02 (t, J= 10.4 Hz, 1 H, H₆), 3.93 (dt, J= 9.5, 6.9 Hz, 1 H, OCH₂), 3.82 (t, J= 9.1 Hz, 1 H, H₃), 3.77 (td, J= 9.1, 1.9 Hz, 1 H, H₅), 3.64–3.50 (m, 3 H, H₂ H₄ OCH₂), 2.97 (br s, 1 H, OH), 2.69 (br s, 1 H, OH), 1.75–1.58 (m, 2 H), 1.37 (m, 8 H), 0.96 ppm (t, J= 7.3 Hz, 3 H). ¹³C NMR (75 MHz, CDCl₃): δ = 134.3, 131.3, 127.8, 103.4 (C₁), 75.0 (C₄), 74.7 (C₃), 74.2 (C₂), 70.8 (OCH₂), 68.7 (C₅), 64.2 (C₆), 31.9, 29.7, 29.2, 26.0, 22.7, 14.2 ppm. The carbon α to the boron was not observed. ¹¹B NMR (96 MHz, CDCl₃): δ = 27.0 ppm. HRMS (ESI) [M+Na] + calculated for C₁₉H₂₉O₆¹¹BNa 387.1955, found 387.1950.

Octyl-β-D-glucopyranoside 4,6-phenylboronate 1e: 127 mg (98%); white solid; m.p.=172–173 °C. [α]_D=-71 (C 1, CH₂Cl₂). 1 H NMR (400 MHz, CDCl₃): δ =7.81 (d, J=7.1 Hz, 2 H), 7.43 (t, J=7.4 Hz, 1 H), 7.34 (t, J=7.4 Hz, 2 H), 4.42 (d, J=7.7 Hz, 1 H, H₁), 4.27 (dd, J=10.4, 5.3 Hz, 1 H, H₆), 3.98 (t, J=10.4 Hz, 1 H, H₆), 3.95–3.82 (m, 1 H, OCH₂), 3.78 (t, J=9.2 Hz, 1 H, H₃), 3.74 (td, J=9.1, 1.1 Hz, 1 H, H₅), 3.64–3.49 (m, 3 H, H₄ H₂ OCH₂), 2.85 (brs, 1 H, OH), 2.56 (d, J=2.3 Hz, 1 H, OH), 1.64 (quint, J=6.9 Hz, 2 H), 1.40–1.20 (m, 10 H), 0.88 ppm (t, J=6.7 Hz, 3 H). 13 C NMR (101 MHz, CDCl₃): δ =134.3, 131.3, 127.8, 103.4 (C₁), 75.0 (C₃), 74.6 (C₄), 74.2 (C₂), 70.8 (OCH₂), 68.7 (C₅), 64.2 (C₆), 31.9, 29.7, 29.5, 29.3, 26.0, 22.8, 14.2 ppm. The carbon α to the boron was not observed. 11 B NMR (96 MHz, CDCl₃): δ =26.9 ppm. HRMS (ESI) [M+Na] + calculated for C₂₀H₃₁O₆ 11BNa 401.2111, found 401.2106.

Nonyl-β-D-glucoside 4,6 phenyl boronate 1 f: 122 mg (94%); white solid; m.p.=170-172 °C. [α]_D=-76 (C 1, CH₂CI₂). ¹H NMR (400 MHz, CDCI₃): δ =7.84 (d, J=6.5 Hz, 2 H), 7.46 (t, J=7.5 Hz, 1 H), 7.37 (t, J=7.4 Hz, 2 H), 4.45 (d, J=7.7 Hz, 1 H, H₁), 4.31 (dd, J=10.4, 5.4 Hz, 1 H, H₆), 4.02 (t, J=10.4 Hz, 1 H, H₆), 3.93 (dt, J=9.5, 6.9 Hz, 1 H, OCH₂), 3.82 (t, J=9.1 Hz 1 H, H₃) 3.78 (td, J=9.2, 2.2 Hz, 1 H, H₅), 3.66-3.51 (m, 3 H, OCH₂ H₂ H₄), 3.18 (d, J=2.1 Hz, 1 H, OH), 2.92 (d, J=2.6 Hz, 1 H, OH), 1.67 (quint, J=6.8 Hz, 2 H), 1.39-1.25 (m, 12 H), 0.91 ppm (t, J=6.7 Hz, 3 H). ¹³C NMR (101 MHz, CDCI₃) δ 134.3, 131.3, 127.8, 103.4 (C₁), 75.1 (C₃), 74.7 (C₄), 74.2 (C₂), 70.8 (OCH₂), 68.7 (C₅), 64.2 (C₆), 32.0, 29.7, 29.6, 29.5, 29.4, 26.0, 22.8, 14.2 ppm. The carbon α to the boron was not observed. ¹¹B NMR (96 MHz, CDCI₃): δ =28.3 ppm. HRMS (ESI) [M+Na] + calculated for C₂₁H₃₃O₆¹¹BNa, 415.22624, found 415.2265.

Decyl-β-D-glucoside-4, 6 phenyl boronate 1g: 117 mg (96%); white solid; m.p.=154–156 °C. [α]_D=-66 (C 1, CH₂Cl₂). ¹H NMR (400 MHz, CDCl₃): δ =7.83 (d, J=7.9 Hz, 2 H), 7.46 (t, J=7.4 Hz, 1 H), 7.37 (t, J=7.4 Hz, 2 H), 4.45 (d, J=7.7 Hz, 1 H, H₁), 4.30 (dd, J=10.4, 5.3 Hz, 1 H, H₆), 4.01 (t, J=10.4 Hz, 1 H, H₆), 3.92 (dt, J=9.5, 6.9 Hz, 1 H, OCH₂), 3.82 (t, J=8.8 Hz, 1 H, H₃), 3.75 (td, J=9.2, 2.1 Hz, 1 H, H₅), 3.65–3.51 (m, 3 H, OCH₂ H₂ H₄), 3.31 (d, J=2.2 Hz, 1 H, OH), 3.05 (d, J=2.7 Hz, 1 H, OH), 1.67 (quint, J=6.9 Hz, 2 H), 1.33–1.29 (m, 14 H), 0.91 ppm (t, J=6.8 Hz, 3 H). ¹³C NMR (101 MHz, CDCl₃): δ =134.3, 131.3, 127.8, 103.4 (C₁), 75.1 (C₃), 74.6 (C₄), 74.2 (C₂), 70.8 (OCH₂), 68.7 (C₅), 64.2 (C₆), 32.0, 29.7, 29.7 (2C), 29.5, 29.4, 26.0, 22.8, 14.2 ppm. The carbon α to the boron was not observed. ¹¹B NMR (96 MHz, CDCl₃): δ =27.5 ppm. HRMS (ESI) [M+Na] + calculated for C₂₂H₃₅O₆¹¹BNa 429.2424, found 429.2419.

Dodecyl-β-D-glucoside-4, 6 phenyl boronate **1 h**: 126 mg (99%); white solid; m.p. = 134–136 °C. [α]_D = -64 (C 1, CH₂Cl₂). ¹H NMR (400 MHz, CDCl₃): δ = 7.83 (d, J = 7.4 Hz, 2 H), 7.47 (t, J = 7.3 Hz, 1 H), 7.37 (t, J = 7.4 Hz, 2 H), 4.45 (d, J = 7.7 Hz, 1 H, H₁), 4.32 (dd, J = 10.4, 5.4 Hz, 1 H, H₆), 4.02 (t, J = 10.4 Hz, 1 H, H₆), 3.93 (dt, J = 9.6, 6.8 Hz, 1 H, OCH₂), 3.80 (t, J = 9.2 Hz, 1 H, H₃), 3.76 (t, J = 9.2 Hz, 1 H, H₅), 3.62–3.54 (m, 3 H, H₂ H₄ OCH₂), 2.99 (brs, 1 H, OH), 2.72 (brs, 1 H, OH), 1.67 (quint, J = 7.1 Hz, 2 H), 1.29 (m, 18 H), 0.91 ppm (t, J = 6.7 Hz, 3 H). ¹³C NMR (101 MHz, CDCl₃): δ = 134.3, 131.3, 127.8, 103.4 (C₁), 75.1 (C₃), 74.7 (C₄), 74.3 (C₂), 70.8 (OCH₂), 68.7 (C₅), 64.2 (C₆), 32.1, 29.8₀, 29.7₈, 29.7₄ (2C), 29.7₀, 29.5₄, 29.5₀, 26.1, 22.8, 14.3 ppm. The carbon α to the boron was not observed. ¹¹B NMR

(96 MHz, CDCl₃): δ = 27.2 ppm. HRMS (ESI) [*M*+Na]⁺ calculated for $C_{24}H_3O_6^{11}BNa$ 457.2737, found 457.2732.

Gel formation

The gels were prepared by mixing the appropriate amount of gelator into the appropriate organic solvent at various percentages in capped tubes. The tubes were heated at $60\,^{\circ}\text{C}$ (cyclohexane), $80\,^{\circ}\text{C}$ (toluene) or $120\,^{\circ}\text{C}$ (fatty esters) for 1 h or until clear solutions were obtained. Clear solutions were then cooled down to room temperature to allow the formation of a gel.

Rheology

Organogel samples were presented under disc form (4 cm diameter). Rheological measurements were performed on an Anton-Paar MCR301 equipped with an upper plate of 75 mm diameter. The frequency (ω) was fixed to 1 Hz and the amplitude deformation (γ °) was gradually increased from 0 to 50% of shearing. Storage modulus G′ and the loss modulus G″ were obtained at 25°C.

Scanning electron microscopy (SEM)

Metalization by Au/Pd. Scanning Electron Microscopy (SEM) of xerogels were evaluated using the JEOL IT 300 Scanning Electron Microscope. Samples were collected and deposited on a Teflon plot. Each sample was examined using a voltage of 5 or 10 kV. Images were analyzed by SMileView software.

Small angle X-ray scattering (SAXS)

Organogel and xerogel samples were prepared into capillaries. SAXS experiments were performed using X-ray patterns collected with a Pilatus 300k (Dectris, Grenoble, France), mounted on a microsource X-ray generator GeniX 3D (Xenocs, Sassenage, France) operating at 30 watts. The monochromatics $\text{Cu}_{\text{K}\alpha}$ radiation is of $\lambda=1.541$ Å. The diffraction patterns were therefore recorded for reciprocal spacing $q=4\pi\times\sin\theta/\lambda$ in a range of repetitive distances from 0.015 Å $^{-1}$ (418 Å) and 1.77 Å $^{-1}$ (3.5 Å). Images were transformed to graphics using the software program Fit2D (ESRF).

Molecular modeling

Cartoon representation of the self-assembly of the organogelators were obtained from the assembly of one molecule previously minimized. These preliminary minimizations were carried out in vacuum, in periodic boundaries and standard conditions taking into account Coulomb and van der Waals interactions; with semi-empirical and restricted Hartree–Fock method, AM1^[18] coupled with an AMBER^[19] force field; version for YASARA software^[20] (YAMBER03). Assembly of several molecule and final representation were obtained using Samson software.^[21]

Acknowledgements

We acknowledge the Ministère de l'Education Nationale, de la Recherche et de la Technologie. The authors thank F. Goutte-fangeas and L. Joanny from the CMEBA (Centre de Microscopie Electronique à Balayage et microAnalyse, Rennes) for assistance in recording the SEM images.

Chem. Eur. J. **2020**, *26*, 13927 – 13934 **www.chemeurj.org** 13933 © 2020 Wiley-VCH GmbH



Conflict of interest

The authors declare no conflict of interest.

Keywords: alkylglucosides · boronates · glycolipids organogels · water sensitive

- [1] a) M. George, R. G. Weiss, Acc. Chem. Res. 2006, 39, 489-497; b) A. Ajayaghosh, V. K. Praveen, Acc. Chem. Res. 2007, 40, 644-656.
- [2] Y. Ohsedo, Polym. Adv. Technol. 2016, 27, 704-711.
- [3] J. H. Jung, S. Shinkai, Top. Curr. Chem. 2005, 248, 223-260.
- [4] a) S. Uzan, D. Barış, M. Çolak, H. Aydın, H. Hoşgören, Tetrahedron 2016, 72, 7517–7525; b) R. Swati, K. Ankaj, P. Vinay, World J. Pharm. Pharm. Sci. 2014, 4, 455–471; c) K. J. Skilling, F. Citossi, T. D. Bradshaw, M. Ashford, B. Kellam, M. Marlow, Soft Matter 2014, 10, 237–256; d) C. L. Esposito, P. Kirilov, V. G. Roullin, J. Controlled Release 2018, 271, 1–20.
- [5] a) G. Aykent, C. Zeytun, A. Marion, S. Özçubukçu, Sci. Rep. 2019, 9, 4893; b) M. D. Segarra-Maset, V. J. Nebot, J. F. Miravet, B. Escuder, Chem. Soc. Rev. 2013, 42, 7086–7098; c) X. D. Yu, L. M. Chen, M. M. Zhang, T. Yi, Chem. Soc. Rev. 2014, 43, 5346–5371; d) X. Yang, G. Zhang, D. Zhang, J. Mater. Chem. 2012, 22, 38–50.
- [6] a) C. Peyrot, P. Lafite, L. Lemiègre, R. Daniellou in Carbohydrate Chemistry: Chemical and Biological Approaches, Vol. 43 (Eds.: A. P. Rauter, T. Lindhorst, Y. Queneau), The Royal Society of Chemistry, Cambridge, 2018, pp. 245–265; b) K. Soundarajan, M. Rajasekar, T. M. Das, Mater. Sci. Eng. C 2018, 93, 776–781.
- [7] a) A. Prathap, K. M. Sureshan, Langmuir 2019, 35, 6005-6014; b) N. Basu, A. Chakraborty, R. Ghosh, Gels 2018, 4, 52; c) I. S. Okafor, G. Wang, Carbohydr. Res. 2017, 451, 81-94; d) C. Lin, S. Maisonneuve, R. Metivier, J. Xie, Chem. Eur. J. 2017, 23, 14996-15001; e) A. M. Vibhute, V. Muvvala, K. M. Sureshan, Angew. Chem. Int. Ed. 2016, 55, 7782-7785; Angew. Chem. 2016, 128, 7913-7916; f) K. Soundarajan, R. Periyasamy, T. Mohan Das, RSC Adv. 2016, 6, 81838-81846; g) A. Vidyasagar, K. Handore, K. M. Sureshan, Angew. Chem. Int. Ed. 2011, 50, 8021-8024; Angew. Chem. 2011, 123, 8171-8174; h) S.-i. Kawano, S.-i. Tamaru, N. Fujita, S. Shinkai, Chem. Eur. J. 2004, 10, 343-351; i) N. Yan, G. He, H. Zhang, L. Ding, Y. Fang, Langmuir 2010, 26, 5909-5917; j) F. Ono, O. Hirata, K. Ichimaru, K. Saruhashi, H. Watanabe, S. Shinkai, Eur. J. Org. Chem. 2015, 6439-6447; k) G. Hibert, M. Fauquignon, J. F. Le Meins, D. Pintori, E. Grau, S. Lecommandoux, H. Cramail, Soft Matter 2019, 15, 956-962.
- [8] a) N. Fujita, S. Shinkai, T. D. James, Chem. Asian J. 2008, 3, 1076–1091;
 b) R. Nishiyabu, Y. Kubo, T. D. James, J. S. Fossey, Chem. Commun. 2011,
 47, 1124–1150; c) S. D. Bull, M. G. Davidson, J. M. H. van den Elsen, J. S. Fossey, A. T. A. Jenkins, Y.-B. Jiang, Y. Kubo, F. Marken, K. Sakurai, J. Zhao, T. D. James, Acc. Chem. Res. 2013, 46, 312–326.
- [9] a) W. Zhai, X. Sun, T. D. James, J. S. Fossey, Chem. Asian J. 2015, 10, 1836–1848; b) X. Wu, Z. Li, X.-X. Chen, J. S. Fossey, T. D. James, Y.-B.

- Jiang, Chem. Soc. Rev. 2013, 42, 8032–8048; c) W. M. J. Ma, M. P. Pereira Morais, F. D'Hooge, J. M. H. van den Elsen, J. P. L. Cox, T. D. James, J. S. Fossey, Chem. Commun. 2009, 532–534; d) X. Sun, T. D. James, Chem. Rev. 2015, 115, 8001–8037.
- [10] R. S. Mancini, J. B. Lee, M. S. Taylor, J. Org. Chem. 2017, 82, 8777-8791.
- [11] a) A. Tsuge, R. Kamoto, D. Yakeya, K. Araki, Gels 2019, 5, 45; b) Y. Kubo,
 W. Yoshizumi, T. Minami, Chem. Lett. 2008, 37, 1238-1239; c) T. Kimura,
 T. Yamashita, K. Koumoto, S. Shinkai, Tetrahedron Lett. 1999, 40, 6631-6634; d) N. Luisier, K. Schenk, K. Severin, Chem. Commun. 2014, 50, 10233-10236.
- [12] a) C. Zhou, W. Gao, K. Yang, L. Xu, J. Ding, J. Chen, M. Liu, X. Huang, S. Wang, H. Wu, Langmuir 2013, 29, 13568–13575; b) N. Kameta, M. Masuda, T. Shimizu, Chem. Commun. 2015, 51, 11104–11107; c) N. Kameta, K. Ishikawa, M. Masuda, T. Shimizu, Langmuir 2013, 29, 13291–13298; d) N. Kameta, K. Ishikawa, M. Masuda, M. Asakawa, T. Shimizu, Chem. Mater. 2012, 24, 209–214.
- [13] a) A. Chen, I. S. Okafor, C. Garcia, G. Wang, Carbohydr. Res. 2018, 461, 60–75; b) A. Chen, L. P. Samankumara, C. Garcia, K. Bashaw, G. Wang, New J. Chem. 2019, 43, 7950–7961; c) G. Wang, A. Chen, H. P. R. Mangunuru, J. R. Yerabolu, RSC Adv. 2017, 7, 40887–40895; d) J. Kowalczuk, M. Bielejewski, A. Lapinski, R. Luboradzki, J. Tritt-Goc, J. Phys. Chem. B 2014, 118, 4005–4015; e) J. Tritt-Goc, J. Kowalczuk, Langmuir 2012, 28, 14039–14044; f) K. Sakurai, Y. Jeong, K. Koumoto, A. Friggeri, O. Gronwald, S. Sakurai, S. Okamoto, K. Inoue, S. Shinkai, Langmuir 2003, 19, 8211–8217; g) H. Xu, J. Song, T. Tian, R. Feng, Soft Matter 2012, 8, 3478–3486; h) J. Morris, P. Kozlowski, G. Wang, Langmuir 2019, 35, 14639–14650; i) O. Gronwald, S. Shinkai, Chem. Eur. J. 2001, 7, 4328–4334
- [14] A. Jacquemet, C. Mériadec, L. Lemiègre, F. Artzner, T. Benvegnu, *Langmuir* 2012, 28, 7591 7597.
- [15] J. N. Israelachvili, Intermolecular and Surface Forces, Academic Press, San Diego, 2011.
- [16] D. Heß, P. Klüfers, Carbohydr. Res. 2011, 346, 1752–1759.
- [17] R. J. Ferrier, J. Chem. Soc. 1961, 2325 2330.
- [18] M. J. S. Dewar, E. G. Zoebisch, E. F. Healy, J. J. P. Stewart, J. Am. Chem. Soc. 1985, 107, 3902–3909.
- [19] a) D. A. Pearlman, D. A. Case, J. W. Caldwell, W. S. Ross, T. E. Cheatham, S. DeBolt, D. Ferguson, G. Seibel, P. Kollman, Comput. Phys. Commun. 1995, 91, 1-41; b) W. D. Cornell, P. Cieplak, C. I. Bayly, I. R. Gould, K. M. Merz, D. M. Ferguson, D. C. Spellmeyer, T. Fox, J. W. Caldwell, P. A. Kollman, J. Am. Chem. Soc. 1995, 117, 5179-5197.
- [20] E. Krieger, G. Vriend, *Bioinformatics* **2014**, *30*, 2981 2982.
- [21] https://www.samson-connect.net.

Manuscript received: April 22, 2020 Revised manuscript received: June 10, 2020 Accepted manuscript online: June 24, 2020 Version of record online: September 29, 2020

Chem. Eur. J. **2020**, *26*, 13927 – 13934 **www.chemeurj.org** 13934 © 2020 Wiley-VCH GmbH